

Density patterns induced by small moonlets in Saturn's rings?

F. Spahn¹ and M. Sremčević²

¹ Institute of Physics, University Potsdam, 14415 Potsdam, Germany

² Faculty of Physics, University Belgrade, 11000 Belgrade, Yugoslavia

Received 29 February 2000 / Accepted 8 March 2000

Abstract. An extension of the model of the gravitational scattering by moonlets in planetary rings to collisional diffusion is presented. The resulting typical propeller-shaped structures bear the chance to deduce the existence of larger (> 100 meter) embedded bodies in planetary rings. Their spatial extensions provide estimates for the size of the embedded bodies and they contain information about the physical properties of the surrounding ring-material like the kinematic viscosity, mass-density, mean free path and collision frequency. The induced structures lie in the range of the resolution of the Cassini Imaging experiment, and thus, could be observed in near future.

Key words: planets and satellites: individual: rings – diffusion – hydrodynamics – scattering

1. Introduction

Hénon (Hénon 1981) suggested that big bodies in planetary rings, from house-sized up to kilometers in size, could cause density features, recording in this way the upper part of the size-distribution of the ring-particles. One famous example of the prediction of the existence of such a body by inspecting the features in the rings is the detection of the satellite Pan in the Encke-division of Saturn's A ring. At first theoretical studies (Cuzzi & Scargle 1985; Showalter et al. 1986) predicted the existence of a moonlet, and later on a careful inspection of the imaging-data (Showalter 1991) confirmed this prediction - the smallest satellite in the Saturn-system, Pan, was found.

A related example in “detecting indirectly the invisible” had been the prediction of absorption features in the plasma environment of Saturn caused by rings or satellites, which also offered the possibility to deduce their existence from the plasma-data of Pioneer 11 (van Allen 1982). In this context, it is supposed that some of the microsignatures of the phase-space density of charged particles in the vicinity of the F ring sampled by Pioneer

11 might be due to a few moonlets which could be too small to have been detected in the Voyager images.

Following these ideas we performed Markov-chain models (Spahn & Wiebicke 1989) in order to describe the gravitational scattering of the ring material by embedded moonlets to obtain the related structures. By analyzing the Voyager UVS occultation data we tried to find such theoretically predicted radial structures (Spahn & Sponholz 1989). The major flaws of these models had been the neglect of dissipative effects like viscous diffusion caused by the collisions between the ring-particles and the restriction to radial density features.

The major goal of this paper is to overcome these shortcomings and to revisit moonlet-induced structures. In Sect. 2 we present an extended model where collisional effects are taken into account in the evolution of a thin dense planetary ring which accommodates a larger body (moonlet). Furthermore, different assumptions for the kinematic viscosity in dense planetary rings are discussed. In Sect. 3 we summarize the results and investigate the dependence of the shape and the length scales of ring-structures on the mass of the embedded body. Finally, we conclude in Sect. 4.

2. Model assumptions

2.1. Balance laws

The dynamics of the model-ring is governed by the conservation of mass and momentum described by the continuity equation and the Navier-Stokes equation, respectively:

$$\partial_t \sigma + \nabla \cdot \{ \sigma \mathbf{u} \} = 0 \quad (1)$$

$$\partial_t \mathbf{u} + (\mathbf{u} \cdot \nabla) \mathbf{u} + \nabla V - \frac{1}{\sigma} \nabla \cdot \hat{\mathbf{P}} = 0. \quad (2)$$

Here σ and \mathbf{u} are the surface density and the mean velocity of the granular flow, V is the gravitational field with its contributions from the planet, an embedded moonlet and the selfgravity of the ring. The pressure tensor is given by

$$\hat{\mathbf{P}} = -p \hat{\mathbf{I}} + 2\sigma\nu \hat{\mathbf{D}} - \frac{2}{3}\sigma\nu \nabla \cdot \mathbf{u} \hat{\mathbf{I}} + \sigma\zeta \nabla \cdot \mathbf{u} \hat{\mathbf{I}}, \quad (3)$$

with the shear tensor

$$\hat{\mathbf{D}} = \frac{1}{2} [\nabla \circ \mathbf{u} + \mathbf{u} \circ \nabla], \quad (4)$$

Send offprint requests to: F. Spahn

Correspondence to: F. Spahn, Universität Potsdam, Institut für Physik, Lehrstuhl Nichtlineare Dynamik, Am Neuen Palais 10, Haus 19, 14415 Potsdam, Germany (Tel. +49 331 977 1626; Fax. +49 331 977 1142; e-mail: fspahn@agnld.uni-potsdam.de)

and the unit-tensor $\hat{\mathbf{I}}$. The vertically integrated pressure, kinematic shear- and bulk-viscosities are given by $p = \sigma c_0^2$, ν , and ζ , with the velocity dispersion $|c_0|$ characterizing the modulus of deviations of the velocity apart from the mean value \mathbf{u} .

In the following simplified model we focus on the effect of the shear-viscosity ν and we neglect the influences of pressure gradient and the bulk-viscosity ζ . These are good approximations as long as all density gradients are rather small and the flow is almost Keplerian giving $\nabla \cdot \mathbf{u} = 0$, which is certainly the case beyond the Hill sphere of gravitational influence of the moonlet.

Provided these assumptions, the remaining problem is to find the flow field \mathbf{u} in the vicinity of the embedded moonlet? One way would be to solve numerically the hydrodynamic Eqs. (1)-(2), which means to discretize the rather small region of gravitational influence of the moonlet, which is numerically very time - and memory consuming. In this paper we deal with bodies of a diameter $D \approx 0.1 \dots 10$ km, where their range of gravitational influence, the Hill-sphere radius $h = r_0 (\mu / [3(1 + \mu)])^{1/3} \approx 3D/2$ (r_0 - radial distance moonlet-planet, $\mu = M_m/M_p$ - ratio between the masses of the moonlet and the planet), is of the order of the size of an icy moonlet itself - a negligible small distance compared to the whole circumference of the ring.

Thus, here we use another method, which we derived already in kinematic models of the gravitational influence of embedded moonlets (Spahn & Wiebicke 1989). To this aim, the whole area of the ring is divided into two parts. The first one is the *scattering region*, approximated to be a line located at the azimuthal longitude of the moonlet $\Phi = 0$ (cylindrical coordinates r and Φ , co-rotating with the moonlet, are chosen). All results of the gravitational action of the moonlet on the ring particles are assumed to be concentrated on this line.

For the rest of the ring it is assumed that the material moves stationary at Keplerian orbits $\mathbf{u} = r\Omega(r) \mathbf{e}_\Phi + u_r \mathbf{e}_r$ ($\Omega(r)$ - Keplerian orbit frequency, u_r - radial velocity), with $|u_r/(r\Omega)| \ll 1$. Provided that \mathbf{u} does not depend on Φ and the selfgravity is neglected, the azimuthal component of the momentum balance reads (Stewart et al. 1984)

$$r u_r \sigma = -3 \partial_r (r^2 \Omega \nu \sigma) / (r \Omega). \quad (5)$$

Inserting this in the continuity equation, where one term of the divergence reads $r^{-1} \partial_r [r u_r \sigma]$, results in a diffusion-type equation. With these assumptions, the mass conservation at the scattering line and in the rest of the ring can be expressed by the Eqs.:

$$r \Omega(r) \sigma(t, r, \Phi = 0) = \int_0^\infty dr' \hat{\mathbf{a}}(r, r') r' \Omega(r') \sigma(t, r', \Phi = 0) \quad (6)$$

$$\partial_t \sigma + (\Omega - \Omega_0) \partial_\Phi \sigma - \frac{3}{r} \partial_r [(r \Omega)^{-1} \partial_r (r^2 \Omega \nu \sigma)] = 0. \quad (7)$$

In Eq. (6) the gravitational scattering is modeled as a Markov process, where the kernel $\hat{\mathbf{a}}$ is the transition probability density

of matter to be scattered from r' to r . This integral equation is approximated by a radial discretization resulting in a matrix equation. In order to get an expression for the scattering matrix corresponding to the kernel $\hat{\mathbf{a}}(r, r')$, the Eqs. of motion of the restricted three-body problem (RTB-problem) have been integrated numerically. A detailed description of calculating the scattering operator is given in (Spahn & Wiebicke 1989), here we report just briefly the technique we have used. In order to derive the transition-probabilities, about 6.5 million test-particles are initially distributed homogeneously in the ring. The eccentricities (thermal velocities) have been chosen out of a distribution (Petit & Hénon 1987) $dp(e) = (2e de/e_0^2) \exp[-e^2/(e_0^2)]$, which corresponds to a stationary velocity dispersion of $c_0 = 0.2 \text{ cm s}^{-1}$ (or $e_0 \approx 10^{-7}$), a value obtained by numerical experiments (Salo 1991; Salo 1992; Schmidt et al. 1999). Then, the changes of the orbital elements of the particles, caused by a single scattering process at the moonlets longitude, have been calculated (Spahn & Wiebicke 1989) and then been used to derive the kernel $\hat{\mathbf{a}}$.

The continuity equation (7) has been solved with a difference method, where the dominant motion - second term in Eq. (7) - is just the differential rotation, and the third term represents the nonlinear viscous diffusion.

2.2. The kinematic viscosity

The crucial value for the viscous diffusion is the kinematic viscosity ν . Analytical (Goldreich & Tremaine 1978; Araki & Tremaine 1986) and numerical (Wisdom & Tremaine 1988; Salo 1991; Salo 1992; Salo 1995) studies yielded $\nu = K(\sigma/\sigma_0)^\beta \nu_0$, with $\nu_0 \propto c_0^2/\Omega_0$, $\beta \approx 1$ and a factor K . However, the viscosity ν as well as the related quasi-equilibrium velocity dispersion $|c_0|$ depend sensitively on processes of how energy is dissipated during particle-collisions (Spahn et al. 1995). The value which characterizes these processes is the coefficient of restitution ϵ , which measures the damping of the thermal motion due to inelastic collisions between the ring-particles (Bridges et al. 1984; Brilliantov et al. 1996). In addition, particles of different sizes also affect the transport processes in planetary rings. The particle-size in planetary rings range from micrometer up to house-size or even kilometer-sized moonlets (satellite Pan in the Encke-division of Saturn's rings). In the size range between centimeter and 5 meter, a size distribution $dN/dR_p \propto R_p^{-\gamma}$, with $\gamma \approx 3$, has been measured by the Voyager radio-science experiments (RSS) (Marouf et al. 1983). Finally, also the gravitational interactions between the ring-particles as well as the selfgravity may have an essential influence on the velocity dispersion and on the kinematic viscosity of planetary rings. All these complex processes, especially the lack of knowledge about the mechanical properties of the ring-particles, give the factor K a wide range of possible values. In a series of numerical experiments Salo (Salo 1991; Salo 1992; Salo 1995) has studied carefully all of these effects, and he obtained $|c_0| \approx (1 - 6) R_p \Omega$

related to viscosities $\nu \approx (1-40)R_p^2\Omega$. The dispersion of K is mainly determined by the parameters of the collision law and of the size-distribution. In the case of gravity and selfgravity (gravitational wakes) these values can well rise up to $|c_0| \approx 15 R_p \Omega$ and $\nu > 100R_p^2\Omega$ (Salo 1995). Here, we have taken $\nu = 10 \text{ cm}^2\text{s}^{-1}$ which corresponds to a dense ring (B ring of Saturn) of quite inelastically behaving, centimeter-sized particles (icy particles with frost-layers, brittle fractures, cracks a.s.o; Salo 1992; Schmidt et al. 1999). These small particles contribute the majority to the optical depth in rings in the case of the given size-distribution, and thus, it is the fraction of the ring-ensemble which will be most probably observed by the Cassini-cameras in 2004. Anyhow, as we will see below, a scaling relation of the structures could serve as a tool to measure indirectly the viscosity in the ring by analyzing the Cassini-images of rings. Thus, for the moment we accept the remaining quite large uncertainties of the value ν and proceed with the coefficient given above. Finally, all results can be scaled to different values of the viscosity as discussed below.

3. Results

We have used values which are adequate to the environment of Saturn's B ring: $r_0 = 10^{10} \text{ cm}$, $\sigma_0 = 100 \text{ g cm}^{-2}$, $\Omega_0 \approx 1.93 \times 10^{-4} \text{ s}^{-1}$. Then, the evolution of the system has been followed by solving numerically Eqs. (6)-(7).

A stationary state establishes as a result of the balance between creation of structures due to the gravitational scattering and their viscous dissipation. Examples of typical structures are shown in Fig. 1 where the stationary density patterns are plotted. These patterns are caused by icy moonlets of sizes $D = 200 \text{ m}$ (top), and 2 km (bottom), respectively. According to this, two different types of structures, depending on the size (mass) of the embedded body, evolve: 1.) Density depletions which can not get around the whole circumference - giving the structure a "propeller-like" appearance (top of Fig. 1); 2.) A gap, not necessarily empty, is formed in the whole ring (bottom of Fig. 1).

For given ring properties the mass of the moonlet is decisive of whether the propeller-structure or a circumferential density depletion will evolve.

For an estimate of the critical size of the moonlet, which separates both structural types, the time- and length scales of the competing processes – gravitational scattering and diffusion – are of importance. It is found that the radial scales of the moonlet-induced density depletions are about $h \propto \mu^{1/3}$ for moonlets smaller than 3 km (Petit & Hénon 1988; Spahn & Sponholz 1989). The synodic period for a distance h from the moonlet is $t_{\text{syn}}(r) = 2\pi/(\Omega(r) - \Omega_0) \approx 4\pi r_0/(3\Omega_0 h)$ which is the time the density features need to get around the whole circumference of the ring.

The characteristic time for the competing process, the viscous diffusion, is $t_\nu \approx |\Delta r|^2/[3(1+\beta)\nu_0]$. The factor $(1+\beta)^{-1}$ arises from the density dependence of $\nu(\sigma)$ in Eq. (7). This estimation just holds for small density gradients and if curvature terms can be neglected.

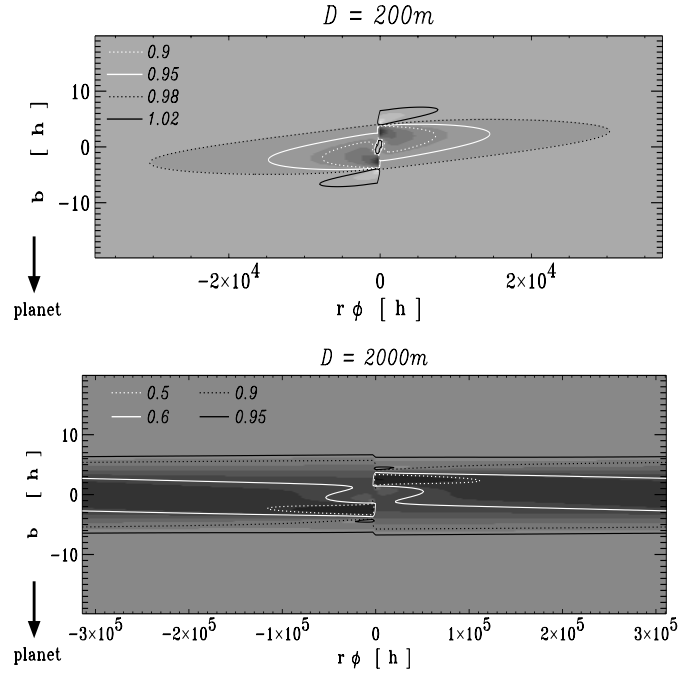


Fig. 1. *Top:* Grey-level presentation of the stationary density of a ring with an embedded moonlet of a size $D = 200 \text{ m}$ showing the typical "propeller" structure. *Bottom:* The same for a moonlet of 2 km in diameter resulting in a circumplanetary density depletion or gap. In both cases an initial optical depth $\tau = 1$ and a viscosity $\nu = 10 \text{ cm}^2\text{s}^{-1}$ have been chosen. The radial variable b , $r = r_0 + bh$ is used. Note that this coordinate is enlarged by factor 10^3 and 10^4 for the small - and the big moonlet, respectively

Identifying the diffusion length with the radial extent of the moonlet-induced features $|\Delta r| \approx h$ and taking into account $\Phi_m = |\Omega - \Omega_0| t_\nu \approx [3\Omega_0 h/(2r_0)] t_\nu$, one obtains the azimuthal extent of the structures $\Phi_m \propto [3(1+\beta)\nu_0]^{-1} D^3$. In a dense ring consisting of very inelastically behaving particles ($\langle\epsilon\rangle \approx 0.3\dots 0.4$), where $\nu_0 \approx 10 \text{ cm}^2\text{s}^{-1}$ (Salo 1992; Schmidt et al. 1999), a larger ring-boulder would be able to cause a circumplanetary feature ($\Phi_m = 2\pi$) if its size is $D > 1 \text{ km}$. In "warmer" rings, where the particles collide more elastically ($\langle\epsilon\rangle \approx 0.8$) and where the ensemble follows closely the $\epsilon - \tau$ relation of equilibrium in the rings, the viscosity gets $\nu \approx 200 \text{ cm}^2\text{s}^{-1}$, the corresponding critical size of a moonlet is $D \approx 2.5 \text{ km}$ to open a gap (Lissauer et al. 1981).

The numerical results confirm the scaling relations fairly well, as shown in Fig. 2. The solid line corresponds to the linear case $\beta = 0$, and the over-plotted diamonds represent the results of the numerical solution for this case. The dashed line corresponds to the case $\beta = 5/4$ where the triangles represent the numerical solutions of the full Eqs. (6)-(7), i.e. where curvatures and density gradients are taken into account.

Up to now, the influence of the moonlet's gravity on the properties of the ring matter (viscosity) has been dropped. In the following we want to give an estimate how the moonlet affects the adjacent ring-material. Beyond the radial borders of the propeller-like structures $|r - r_0| \geq 5h$, the moon-

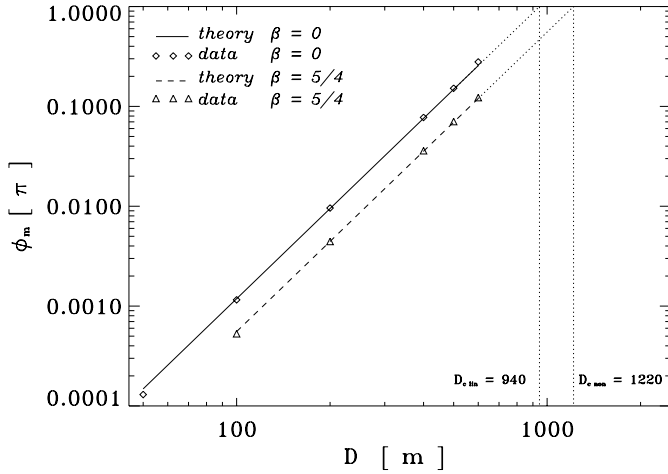


Fig. 2. A log-log plot of the azimuthal extent Φ_m versus the size of the moonlet D , which confirms the scaling $\Phi_m \propto D^3$ for $\beta = 0$ as well as for $\beta = 5/4$. According to this, the critical size for a moonlet to produce a circumferential feature is $D_c \approx 1.22$ km.

let induces an eccentricity in the orbits of the ring-particles, which is $e_i \approx \mu [r_0/(r - r_0)]^2$ (Showalter et al. 1986). This is the region of density wakes, a collective motion originated by the nearby moonlet. However, after a certain angle $\Phi_s \propto D$ (Showalter et al. 1986; Marouf & Tyler 1986) away from the moonlet, streamlines (mass-loaded virtual lines characterizing the particle motion) start to cross and collisions destroy the in-phase motion and damp the induced eccentricities (Hertzsch et al. 1997). Because this critical angle depends on the size of the moonlet, wakes are only visible in a considerable azimuthal range for large moonlets, e.g. in the case of the satellite Pan ($D \approx 10...15$ km), the azimuthal range of detectability of the wakes is about $O(\pi)$ (Horn et al. 1996). Boulders two orders of magnitude smaller, which we are mainly interested in this paper, do not really form visible wakes because $\Phi_s \ll 1$. Close to the longitude of the small moonlet the collective motion is dissipated simultaneously by two processes: *i*) destruction of the phase relation of the certain orbits of the particles due to collisions; *ii*) damping of the induced eccentricities due to the inelasticity of the collisions (Hertzsch et al. 1997). The first process corresponds to a heating and the latter to a cooling of the particle ensemble. Although cooling and heating act simultaneously for the moment we only discuss the extreme case where the induced eccentricity e_i would be exclusively attributed to a heating of the ring particle ensemble. This would result in an considerable enhancement of the kinematic viscosity according to $\nu_0 \approx \Omega_0 r_0^2 e_i^2 \approx 10^{-1} \Omega_0 D^2$. Again the relations $D \approx 2h/3$, $h/r_0 \approx (\mu/3)^{1/3}$ and $|r - r_0|/h = 5$ are used. This induced velocity dispersion c^2 would exceed considerably the balanced value $c_0^2 \propto (R_p \Omega_0)^2$ found in unperturbed dense rings. How long does it take until these perturbations will be relaxed? The granular cooling will damp out these perturbations in time-scales $t_{\text{relax}} \approx 1/[(1 - \epsilon^2)\Omega_0\tau] \approx O(\Omega_0^{-1}) \ll t_{\text{syn}}$ (Haff 1983; Petzschmann et al. 1999). Here, the optical depth is denoted by $\tau \propto \sigma$. With these assumptions we get the relative

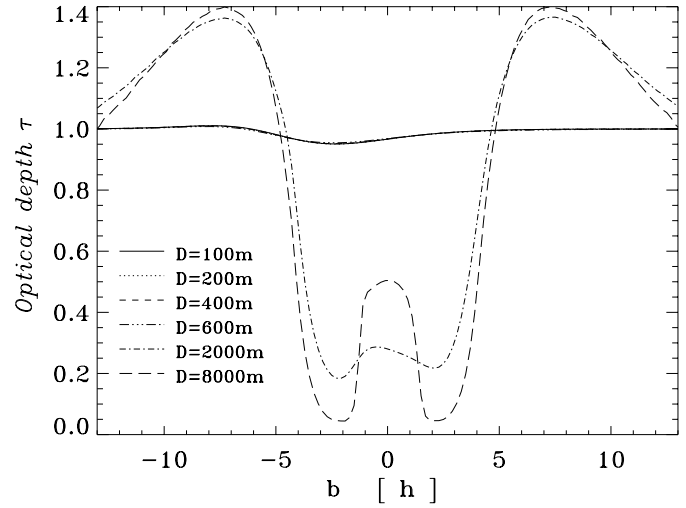


Fig. 3. Radial cuts of the density field at $\Phi = \Phi_m/2$ for the moonlets: $D = 100$ m, 200 m, 400 m, 600 m, 2000 m, and 8000 m. The optical depth profiles turn from a small depletion up to a gap with a weak indication of a ringlet. All cuts of the “propellers” fall nearly on top of each other if they are scanned at the same (scaled by D^3) azimuth $\Phi_m/2$.

change of the width of the density depletion $|\Delta W/W| < 10\%$ caused by the amplified viscous diffusion during this time t_{relax} . Because we have neglected the mere damping of the wakes, which does not contribute to the enhancement of the velocity distribution, the influence of moonlet is even less important for the heating of the ensemble. Thus, we conclude that our simple model should give at least the right order of magnitude of the sizes of the propellers. In a more comprehensive model the energy balance, providing evolution Eqs. for the velocity dispersion c^2 , has to be taken into account (Petzschmann et al. 1999; Schmidt et al. 1999) – a work which is in progress.

4. Discussion

According to the viscous diffusion considered here, only a moonlet with $D > 2$ km can form complete circumferential density structures. Furthermore, density features which have been predicted in previous kinematic studies (Spahn & Sponholz 1989; Spahn & Wiebicke 1989), e.g. the inner ringlet, can only be expected to appear for moonlets larger than 5 km. A dissipation of the inner ringlet is to be expected unless there is a steady material supply by the moonlet, for instance, due to micro-meteorite impact-ejecta (Colwell 1993). Radial cuts of the density field $\sigma(r)$ at the longitude $\Phi = \Phi_{\text{max}}/2$ are shown in Fig. 3 to illustrate these findings. For smaller moonlets ($D < 1$ km) only moderate density depletions are obtained. For larger moonlets double or triple peaks are found which, however, are almost completely smeared out. Furthermore, it has to be noted that the scaling of the width W of the gap according our model (three-body problem) becomes incorrect for $D > 3$ km. Petit and Hénon (Petit & Hénon 1988) showed that the gap width becomes $W \propto h^2$, instead of $W \propto h$ for larger moonlets. This behavior is caused by gravitational

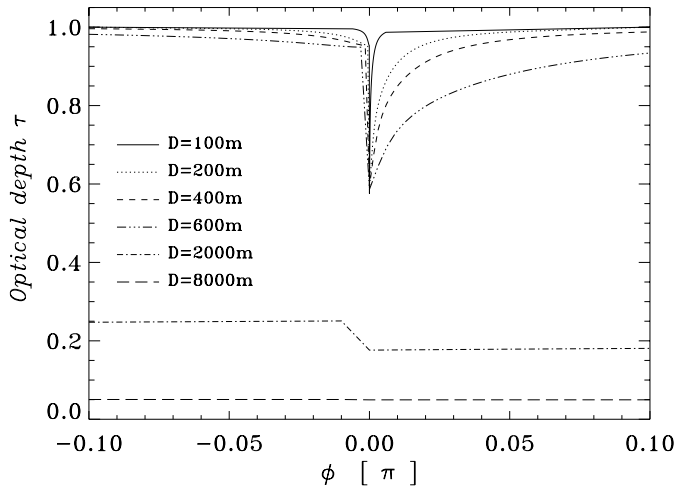


Fig. 4. Azimuthal cuts of the density field, taken at the radial position of the total minimum ($b_{\min} \approx 2h$). Azimuthal features scale with D^3 . Note the abrupt jump of the density at the longitude of the moonlet – an especially useful feature for the detection of such large ring-particles.

back-reaction of the ring-structures onto the orbit of the moon, which is not considered in our model.

Very strong changes in the density have been found in the azimuthal direction around the location of the moonlet of smaller sizes ($D < 1$ km), shown in Fig. 4.

Summarizing: The above features could serve as hints for the Cassini experiments to deduce the size and the distribution of larger bodies indirectly from the optical depth. Especially, the Cassini ring occultations as well as images of the Cassini-cameras will be suitable to recognize the structures related to large bodies. The radial scaling of the size of the moonlet-induced structures can be used to measure the size-distribution of the largest bodies. The azimuthal scaling then provides the possibility to probe properties of the granular matter surrounding the moonlet. In this way the viscosity as a function of density $\nu(\sigma)$ might be estimated from the imaging data of the Cassini spaceprobe, provided that the size of the moonlet is known from the radial extent of the structures.

A more sophisticated model should include the dynamical interaction between the embedded moonlet and the ring-material which modifies the transport properties of the granular matter in the rings. Furthermore, the simplification of the

scattering-process to occur just on a line should be supplemented by direct collisional simulations of the close surrounding of the moonlet.

Acknowledgements. The authors would like to thank the anonymous referee for his helpful comments. This work was supported by the DAAD (Deutscher Akademischer Austauschdienst).

References

- Araki S., Tremaine S., 1986, *Icarus* 65, 83
 Bridges F., Hatzes A., Lin D., 1984, *Nature* 309, 333
 Brilliantov N., Spahn F., Hertzsch J.-M., et al., 1996, *Phys. Rev. E* 53, 5382
 Colwell J., 1993, *Icarus* 106, 536
 Cuzzi J. N., Scargle J. D.: 1985, *ApJ* 292, 276
 Goldreich P., Tremaine S., 1978, *Icarus* 34, 227
 Haff P.K.: 1983, *J. Fluid Mech.* 134, 401
 Hénon M., 1981, *Nature* 293, 33
 Hertzsch J.M., Scholl H., Spahn F., Katzorke I., 1997, *A&A* 320, 319
 Horn L.J., Showalter M.R., Russell C.T., 1996, *Icarus* 124, 663
 Lissauer J.J., Shu F.H., Cuzzi J.N., 1981, *Nature* 292, 707
 Marouf E.A., Tyler G.L., 1986, *Nature* 323, 31
 Marouf E.A., Tyler G.L., Zebker H.A., et al., 1983, *Icarus* 54, 189
 Petit J.M., Hénon M., 1987, *A&A* 173, 389
 Petit J.M., Hénon M., 1988, *A&A* 199, 343
 Petzschmann O., Schwarz U., Spahn F., Grebogi C., Kurths J., 1999, *Phys. Rev. Lett.* 82, 4819
 Salo H., 1991, *Icarus* 90, 254
 Salo H., 1992, *Icarus* 96, 85
 Salo H., 1995, *Icarus* 117, 287
 Schmidt J., Salo H., Petzschmann O., Spahn F., 1999, *A&A* 345, 646
 Showalter M.R., 1991, *Nature* 351, 709
 Showalter M.R., Cuzzi J.N., Marouf E.A., Esposito L.W., 1986, *Icarus* 66, 297
 Spahn F., Sponholz H., 1989, *Nature* 339, 607
 Spahn F., Wiebicke H.J., 1989, *Icarus* 77, 124
 Spahn F., Hertzsch J.-M., Brilliantov N., 1995, *Chaos, Solitons & Fractals* 5, 1945
 Stewart G.R., Lin D.N.C., Bodenheimer P., 1984, In: Greenberg R., Brahic A. (eds.), *Planetary Rings*, Univ. of Arizona Press, Tucson Arizona, p. 447
 van Allen J.A., 1982, *Icarus* 51, 509
 Wisdom J., Tremaine S., 1988, *AJ* 95, 925